University of Wollongong

Research Online

Effects of surface preparation on tribological behaviour of a ferritic stainless steel in hot rolling

Xiawei Cheng
University of Wollongong, xiawei@uow.edu.au

Zhengyi Jiang
University of Wollongong, jiang@uow.edu.au

Dongbin Wei
University of Wollongong, dwei@uow.edu.au

Liang Hao
University of Wollongong, lh421@uowmail.edu.au

Hui Wu
University of Wollongong, hw944@uowmail.edu.au

See next page for additional authors

Recommended Citation

Effects of surface preparation on tribological behaviour of a ferritic stainless steel in hot rolling

Abstract

Some defects on the surface of carbon steel do not need to be removed before hot rolling because the surface will be vigorously oxidised in a reheating environment. Thus the defects can be minimised by oxidising and then removed by the de-scaling process. The defects on the surface of ferritic stainless steels, however, are not easily removed by oxidation when a high chromium concentration is used. In this paper, a ferritic stainless steel grade 445 was selected as a research material. The effects of different surface features on oxidation and tribological behaviour in the hot rolling process were investigated. Three surface states were prepared, namely, smooth surface, surface with 45° grinding marks and surface with oscillation marks. The samples were put into an electric furnace at 1100 °C for reheating. Hot rolling tests were carried out on a 2-high Hille 100 experimental rolling mill. Rolling forces were measured, and the coefficient of friction was calculated and compared under various rolling parameters. It was found that the original surface profiles with grinding marks were still maintained during oxidation. The original oxide scale on the surface with oscillation marks caused the formation of irregular oxide nodules and the spallation of the oxide scale. Surface morphology and the reduction in thickness had a significant impact on the oxide scale integrity and coefficient of friction in the hot rolling process.

Disciplines

Engineering | Science and Technology Studies

Publication Details

Authors

Xiawei Cheng, Zhengyi Jiang, Dongbin Wei, Liang Hao, Hui Wu, Wenzhen Xia, Xin Zhang, Suzhen Luo, and Laizhu Jiang

Effects of surface preparation on tribological behaviour of a ferritic stainless steel in hot rolling

Xiawei Cheng[1], Zhengyi Jiang[1,*], Dongbin Wei[1,2], Liang Hao[1], Hui Wu[1], Wenzhen Xia[1], Xin Zhang[3], Suzhen Luo[3], Laizhu Jiang[3]

[1]School of Mechanical, Materials and Mechatronic Engineering, University of Wollongong, Wollongong, NSW 2522, Australia
[2]School of Electrical, Mechanical and Mechatronic Systems, University of Technology Sydney, NSW 2007, Australia
[3]Baosteel Research Institute (R&D Centre), Baoshan Iron & Steel Co., Ltd., Shanghai 200431, PR China

Abstract

Some defects on the surface of carbon steel do not need to be removed before hot rolling because the surface will be vigorously oxidised in a reheating environment. Thus the defects can be minimised by oxidising and then removed by de-scaling process. The defects on the surface of ferritic stainless steels, however, are not easily removed by oxidation when a high chromium concentration is used. In this paper, a ferritic stainless steel grade 445 was selected as a research material. The effects of different surface features on oxidation and tribological behaviour in hot rolling process were investigated. Three surface states were prepared, namely, smooth surface, surface with 45 ° grinding marks and surface with oscillation marks. The samples were put into an electric furnace at 1100 °C for reheating. Hot rolling tests were carried out on a 2-high Hille 100 experimental rolling mill. Rolling forces were measured, and the coefficient of friction was calculated and compared under various rolling parameters. It was found that the original surface profiles with grinding marks were still maintained during oxidation. The original oxide scale on the surface with oscillation marks caused the formation of irregular oxide nodules and the spallation of the oxide scale. Surface morphology and the reduction in thickness had significant impact on the oxide scale integrity and coefficient of friction in hot rolling process.

Keywords: Ferritic stainless steel; Oxide scale; Reheating; Rolling friction

* Corresponding author. Tel: +61-2-42214545; Fax: +61-2-42215474

E-mail addresses: xc979@uowmail.edu.au (X. Cheng), jiang@uow.edu.au (Z. Jiang)

1. Introduction

Surface defects on carbon steel can be minimised by oxidising and then removed by de-scaling process, thus the surface defects on carbon steel do not need to be removed previously before the slabs are placed into reheating furnace because their surfaces will be vigorously oxidised in a reheating environment [1]. Stainless steels are iron-based alloys that contain a minimum of about 12% Cr. The defects on the surface of some stainless steels, however, are not easily removed by oxidation [2] especially when a high Cr concentration is used. Cr is the main element used in order to induce corrosion resistance in stainless steels. Generally, the higher the Cr concentration, the higher the oxidation resistance is [3-5]. Ferritic stainless steels, containing little or no nickel, although their corrosion resistance is inferior to austenitic stainless steels [6], are widely used because they are cheap [7, 8]. The lower thermal expansion coefficient of the ferritic stainless steel makes them excellent for high-temperature applications with thermal cycles, provided their strength is adequate [2]. Thus more ferritic stainless steel products with a high Cr content are developed and produced. It has been noted that, as the chromium exceeds 20 w.t%, the stainless steels have high oxidation resistance [9, 10], e.g. ferritic stainless steel grades 443 and 445. A defect mark from a slab-heating furnace on such stainless steels will remain through the hot rolling, annealing, and cold rolling process [2]. Thus, a slab grinder will mechanically remove the surface defects on the ferritic stainless steel slab before the steel slab is put into the reheating furnace. The grinding marks caused by a slab grinder will appear on the surface of the slab where there were surface defects, such as small holes, and cracks. Oscillation marks are ripples formed on the surface of continuously cast material. They may cause cracking and decrease the yield of the process since some defects must be ground away to avoid crack growth.

2

The oxide scale on stainless steels exhibits complicated characteristics because the oxidation is significantly affected by the alloying elements and the atmosphere [8]. The two major phases of a stainless steel oxide scale are the M_2O_3 rhombohedral phase (e.g. Cr_2O_3 and Fe_2O_3) and the M_3O_4 spinel phase (e.g. $Fe_xCr_{3-x}O_4$ and $Mn_{1.5}Cr_{1.5}O_4$) [10-13]. Usually, the lower thermal expansion coefficient of ferritic stainless steels makes their oxide scale more compatible with the base substrate and provides them with lesser tendency to spall [3]. It is found that the oxide scale deformation behaviour on carbon steels strongly depends on the rolling temperature and the oxide scale thickness [14]. The oxide scale thickness on carbon steels appears to be more important than the oxide scale composition on friction, and thicker scales give lower friction values [15]. Little is known about effects of the surface preparation on oxidation and deformation behaviour of the stainless steels in hot rolling. The objective of this study is to investigate the surface preparation of the ferritic stainless steel 445, i.e. oxide scale thickness, the surface with or without grinding and oscillation marks on the oxidation behaviour at high temperature and the surface transformation after hot rolling at various reductions in thickness. The morphology of the oxide scale of the strip before and after rolling was analysed. Deformation behaviour of the oxide scale and its effects on friction were also examined and discussed.

2. Experimental details

2.1. Material

A ferritic stainless steel grade 445 was selected in this investigation and its chemical composition is shown in Table 1. All the samples used in the experiment were adopted from hot rolled strips.

Table 1 Chemical composition (wt.%) of the ferritic stainless steel grade 445

C	Si	Mn	P	Cr	Cu	Mo	Ti	Nb	Fe
≤0.01	0.30	≥0.15	0.03	21.50	0.10	0.60	≤0.20	0.12	Bal.

2.2. Oxidation and hot rolling test

The material used was cut from the slab and the specimens without marks were machined to the size of $300(L) \times 100(W) \times 10(H)$ mm^3. The specimens with grinding or oscillation marks were machined to the size of $100(L) \times 125(W) \times 10(H)$ mm^3. In order to assist the sample to be bitten into the roll gap, the front of the specimen was tapered to a thickness of 1 mm. The surfaces without marks of the specimens were ground and the measured surface roughness R_a was 0.25 µm. Small samples of $10(W) \times 10(L) \times 10(H)$ mm^3 were cut from the material with different surface preparation for the oxidation test. Reheating was carried out in a high temperature electric resistance furnace with a chamber size of $350(W) \times 330(H) \times 870 (D)$ mm^3. In general, the water vapour contents between 7.0 and 19.5 vol. % in humid air are considered relevant to hot rolling [16]. Therefore, a water vapour generator was connected to the furnace and 18% water vapour content was selected to flow into the furnace at 15 litres/min.

Hot rolling experiments were carried out on a 2-high Hille 100 experimental rolling mill with rolls of 225 mm diameter and 254 mm roll body length. Rolling forces were measured by load cells on the mill. Rolling speed can be set from 0.12 to 0.72 m/s. The roll speed in the real industry is far faster than that in the laboratory, e.g. the first pass roll speed is 2 m/s in Baosteel, so that the rolling speed was set to a maximum of 0.72 m/s or 60 rpm. Reductions of 20, 30 and 40% were selected for the surfaces without marks. Reductions of 20 and 40% were selected for the surfaces with marks. The specimens without marks were thoroughly cleaned with acetone before reheating, but the specimens with marks were kept as they were. All the specimens were placed immediately in a cooling box with nitrogen gas after hot rolling or reheating to prevent further oxidation.

2.3. Observation and analysis

The surface of the samples was covered with a mixture of epoxy resin and hardener to protect the oxide scale after oxidation. After 24 h the resin coagulated, and then the protected oxide scale part was sectioned along the rolling direction by a Stuers Accutom50 Cutting Machine to obtain the cross-section of the oxide scale. Finally, the oxide scale sample was cold mounted, ground and polished. To analyse the scale cross-section, all oxidised samples were prepared using a technique reported by Chen and Yuen [17] and Wei et al. [18, 19] to minimise preparation damage to the oxide scale.

The microstructures, composition and thickness of the oxide scale were examined by a JEOL JSM 6490 scanning electron microscope (SEM) equipped with an Energy Dispersive Spectrometer (EDS) and backscatter electron imaging (BSE). The surface

profiles were examined using a VHX-1000 digital microscope with 2D/3D imaging and measurement capability. X-ray diffraction was used for the phase identification of the oxide scale.

3. Results and discussion

3.1 The oxide scale with different thickness on the stainless steel 445 and its deformation behaviour in hot rolling

In our previous studies, the oxidation kinetics of the steel 445 was investigated by a thermogravimetric analyser (TGA) at the temperatures of 1000, 1030, 1060, 1090, 1120 and 1150 °C [10]. Before hot rolling the samples were placed in the electric resistance furnace for reheating. We used the maximum operating temperature of this furnace, which is 1100 °C. It is known that Cr_2O_3 would be the main composition of the oxide scale formed at such a temperature. We need to present the cross-sections of the oxide scale formed at different oxidation times because later we adopt different oxide scale thickness on the steel for the hot rolling process.

Fig. 1a-d shows the cross section of the oxide scale when the stainless steel 445 was oxidised at 1100 °C from 30 to 120 min at an interval of 30 min in humid air. Only one layer of oxide scale was formed during 120 min. The thickness of oxide scale was 2.8±0.15 µm when the sample was oxidised for 30 min, then steadily grew to 4.1±0.20 µm for 60 min, over time it reached 6.0±0.26 µm for 120 min and the surfaces became gradually even. The surface morphology of the steel 445 after being oxidised in humid air for 120 min is shown in Fig. 1e. No spallation was observed when the specimen was cooled down to ambient temperature. The cross section of the oxide scale shows that the oxide scale adheres to the steel substrate and it is compact

6

without obvious pores in the oxides. The method of characterising the oxide scale can be found in our previous study [10]. The black spots at the steel/oxide are discontinuous Si-rich oxides. Cheng et al. [9] found that this characterisation of Si only existed when there was no Cr depletion in the steel. The oxide spinels were formed on top of the surface with different sizes as shown in Fig. 1f. The oxide scale is mainly made of Cr_2O_3, as shown by its EDS line analysis in Fig. 1. Cr_2O_3 has a corundum structure, which consists of an hcp array of oxygen with two-thirds of the octahedral sites occupied by the metal [26-28]. EDS spot analysis shows that M in spinel M_3O_4 is comprised of Cr, Mn and small amount of Fe. The mean grain size of the spinels is about 2 µm and the spinels are incorporated into the fine Cr_2O_3 scale. The formation of compact and continuous Mn-Cr spinel on top of the Cr_2O_3 scale on Mo alloying 445 steel greatly reduce the evaporation of chromium species [9], and this causes high oxidation resistance of this stainless steel. The structures and compositions of the oxide scales are similar to that oxidised at 1090 and 1120 °C for 120 min [10], but the thickness is different. The oxidation behaviour is different from carbon steels on which the oxide scale is porous and thick with three oxide layers [20]. When the oxide scale is formed on carbon steel at high temperature, the relative thickness of FeO: Fe_3O_4: Fe_2O_3 are in the ratio of roughly 95:4:1 at 1000 °C [4]. Occurrence of FeO phase accelerates oxidation because this oxide scale contains an excessive number of cation vacancies and a large composition range, which are conducive to rapid diffusion of iron ions across the oxide scale. Therefore, the oxide thickens rapidly at the expense of the metallic phase [21]. However, there was no FeO phase formed on this stainless steel. The density of the oxide scale is a physical property that can demonstrate the voids or pores in the oxide scale. With the same composition, the lower the density the higher the pores in the oxide scale. This
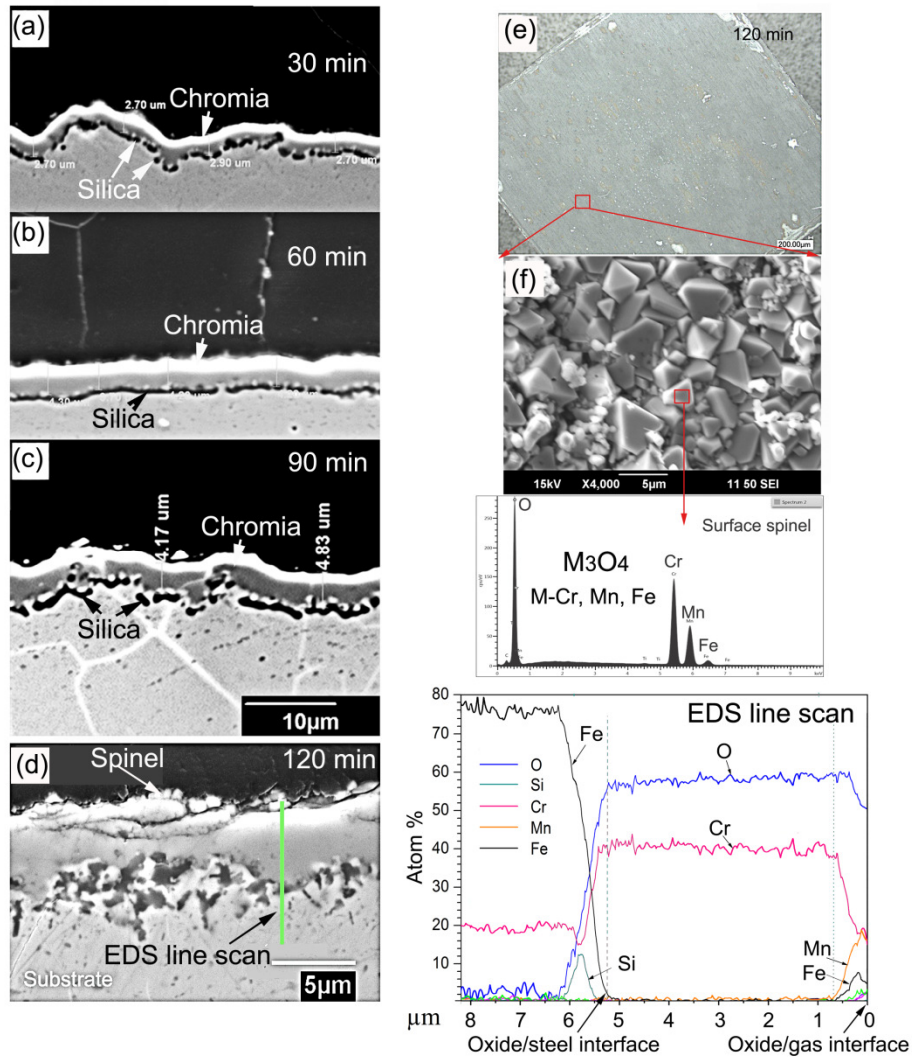
7

Fig. 1 The microstructures of the oxide scale on the stainless steel 445 oxidised from 30 to 120 min in humid air before hot rolling. (a) Cross section of the oxide scale oxidised for 30 min, (b) oxidised for 60 min, (c) oxidised for 90 min, (d) oxidised for 120 min and the result of EDS line scan on the right;, (e) oxidised sample surface, and (f) SEM surface morphology

According to the oxidation study of the stainless steel 445 [10], the oxidation kinetic curves (mass change versus time) of the stainless steel 445 presenting a parabolic law

8

from 1030 to 1120 °C is shown in Fig. 2a. Compliance to the parabolic law indicates that the diffusion of the ions through the oxidised layer was the rate-determining step according to Wagner's theory [3]. No breakaway oxidation occurred at 1100 °C, indicating no iron-rich oxide formed on the stainless steel 445. The high temperature oxidation kinetics of metals or alloys is commonly controlled by the diffusion of cationic or anionic species through the oxide scale [23]. This control leads to a parabolic rate constant, k_p, expressed in $mg^2 /cm^4 /s$, and defined by $(\Delta m/A)^2 = k_p t$ [23], where $\Delta m/A$ is the specific weight gain per area unit [mg/ cm^2], t is the oxidation time (s). The Arrhenius equation can be given in the form:

$$k_p = k_0 \, e^{(-EA/RT)} \qquad (1)$$

where k_0 is the pre-exponential factor of the reaction ($mg^2 /cm^4 /s$), R is the universal gas constant (8.314×10^{-3} kJ/mol/K), T is the temperature in kevin (K) and E_A is the activation energy(kJ /mol). The activation energy obtained from the Arrhenius plot as shown in Fig. 2b is 263 kJ/mol for the formation of the Cr_2O_3 scale in humid air [10]. Then the value of $K_0 = 6.82 \times 10^6$ $mg^2 /cm^4 /s$. Therefore, the ==kinetic== equation can be defined as follows:

$$(\Delta m/A)^2 = 6.82 \times 10^6 \, e^{(-263/RT)} \, t \qquad (2)$$

The parabolic curves from Eq. (2) are plotted in Fig. 2a with solid lines to compare to the experimental results. It can be seen that the curves from Eq. (2) fit the experimental curves. The parabolic curves of the Cr_2O_3 scale growth on the stainless steel 445 at 1000 and 1100 °C were also plotted according to Eq. (2). Table 2 shows

the derived data of the mass gain ($\Delta m/A$) from Eq. (2) when the steel is oxidised at 1100 °C from 30 to 120 min in humid air. With the corresponding thickness at each oxidation time, the density of the Cr_2O_3 scale formed on the steel 445 can be calculated (Δm/A/ξ.). It can be seen from Table 2, that the density of the Cr_2O_3 scale has not changed much over time. This density is less than that of the bulk Cr_2O_3, 5.22 g/cm^3. The impurity and voids by cation diffusion in the oxide scale affect this property greatly.
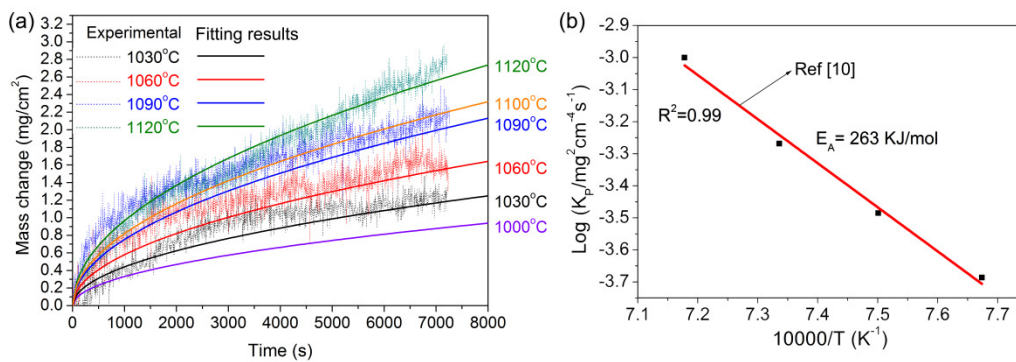

Fig. 2 (a) Mass change versus time curves for the stainless steel 445oxidised for 120 min at different temperatures in humid air [10] and the parabolic curves from the Eq.(2) and (b) Arrhenius plot of oxidation parabolic constants at 1030, 1060, 1090 and 1120 °C for the stainless steel 445 [10].

Table 2 The oxide scale properties formed at different oxidation times at 1100 °C in humid air

Oxidation time(min)	Δm/A(mg/cm^2)	Thickness ξ (µm)	Density (g/cm^3)
30	1.20	2.8±0.15	4.3
60	1.69	4.1±0.20	4.1
90	2.07	5.1±0.12	4.1
120	2.39	6.0±0.26	4.0

Fig. 3 shows the surface morphology of the steel 445 at different reductions in thickness after hot rolling at 1050 °C. The rolling specimens were reheated in an electric furnace at 1100 °C for 120 min in humid air. Fig. 3a shows no cracks on the

surface when the specimen was rolled at the reduction of 19.8%. The surface was covered with fragmented particles. Fig. 3b shows small transverse cracks on the surface but in general, the oxide scale remains integral at the reduction of 29.9%. Fig. 3c shows some big cracks and the cracks are in different directions at the reduction of 39.8%.
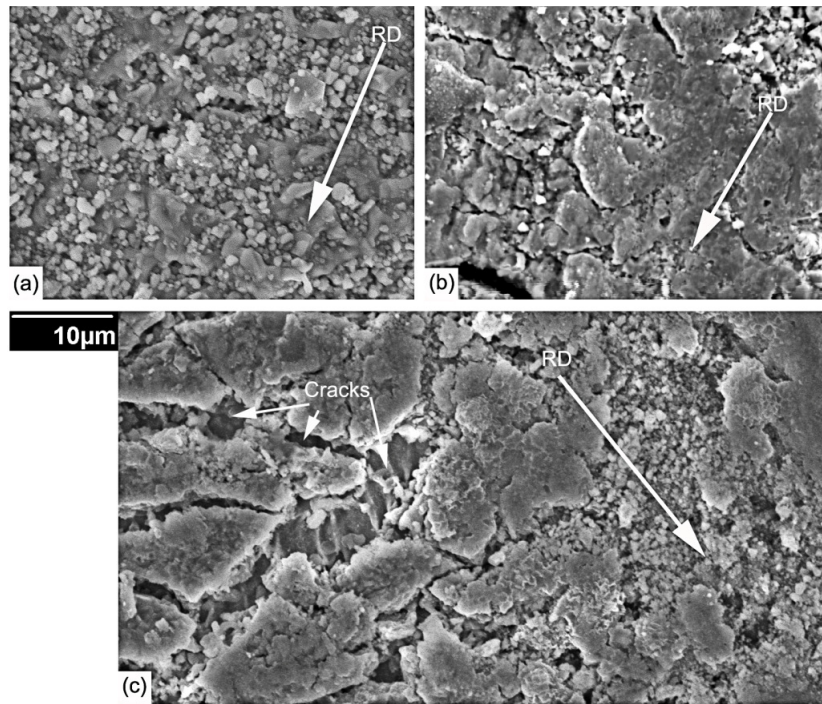

Fig. 3 The surface micrographics of the rolled specimens oxidised for 120 min with a oxide scale thickness of 6.0 ±0.26 µm under different reductions: (a) 19.8%, (b) 29.9%, and (c) 39.8% (Arrows indicate rolling direction (RD))

After hot rolling, the oxide scale on the rolled specimens was not spalled off and adhered to the steel substrate. Fig. 4 shows back-scattered electrons (BSE) images of the cross sections of the rolled specimens at different reductions and the corresponding 3-D surface profiles for the rolled specimens. The surface roughness was conformal to its morphology observed by SEM and 3-D surface profiles. The surface roughness Ra is in the order: 39.8% >19.8% >29.9%. According to the investigation of the Cr_2O_3 scale on the ferritic stainless steel by Cheng et al. [24], the Cr_2O_3 scale is more brittle than the steel substrate and the ductility could be improved

11

with increasing the temperature. Fig. 4a-c shows that, as the reduction in thickness increases from 19.8 to 39.8%, the thickness of the deformed oxide scales decreases. The deformation behaviour of the oxide scale on carbon steel can be characterised as brittle, mixed, or ductile, based on its integrity between 650 and 1050 °C in hot rolling [25]. The oxide scale shows various deformation behaviours [26-29]. Utsunomiya et al. [28] classified them into some categories: (a) uniform deformation with matrix steel, (b) cracking, (c) fragmentation, and (d) indentation to matrix steel, etc. The deformation behaviour of the oxide scale strongly depends on the rolling temperature and the oxide scale thickness [14, 30]. In our study, it can be seen from Fig. 4-c, the steel/oxide interface is not even at different reductions. At 1050 °C, hard brittle oxide was fragmented and indented to the steel substrate so that the interface was rough and this became severe when the reduction is high. As shown in Fig. 4c, when the reduction is 39.8%, the steel substrate is extruded from the through thickness cracks in the oxide scale to the outmost surface.
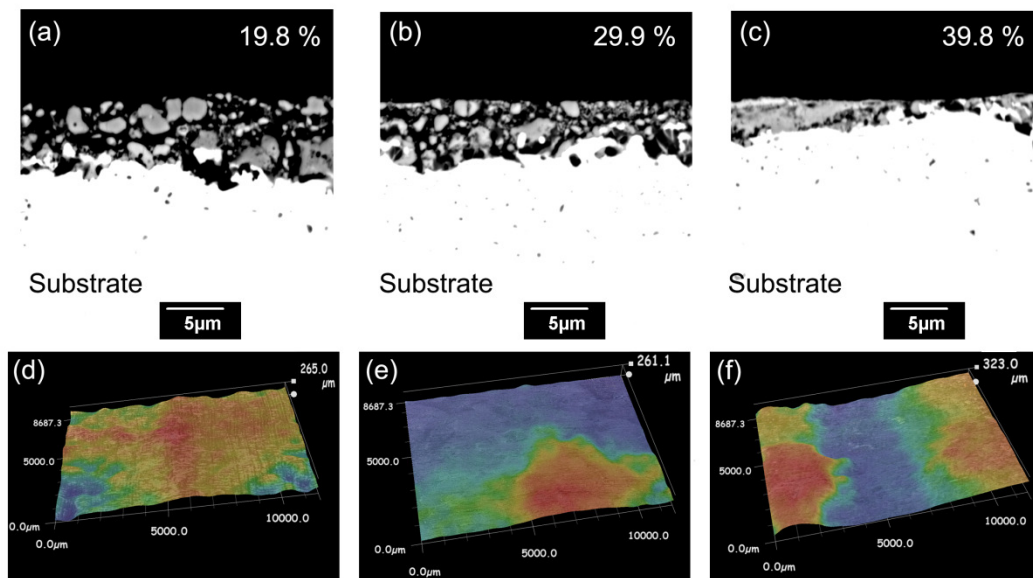

Fig. 4 The cross sections of rolled stainless steel with a thickness of 6.0±0.26 μm under different reductions and corresponding 3-D surface profiles: (a)(d) 19.8%, (b)(e) 29.9%, and (c)(f) 39.8%.

The variation of the roll separating forces through the roll gap at reductions varying from 19.8 to 39.8% is shown in Fig. 5. The thickness of the oxide scale differed by the oxidation time (Table 2). The thickness of the Cr_2O_3 scale has not varied much between 60 (4.1±0.20 µm) and 120 min (6.0±0.26 µm) and the main constitute and its density have not changed over time. The roll separating forces were slightly higher when there was a thin oxide scale on the steel, at reductions ranging from 19.8 to 30.2%. However, the rolling force differences were negligible with an increase of oxide scale thickness at the reduction of approx. 40%. At such a high reduction, wherever the oxide scale thickness was thin or thick, the deformation behaviour of the Cr_2O_3 scale was similar. The Cr-rich oxide scale on the steel rolled at different temperatures showed that its deformation behaviour changed greatly when the rolling temperature changed [24]. The oxide scale is thinner, harder and more brittle at or below 1000 °C than that at 1050 °C. This study shows that a slightly thicker Cr-rich oxide scale with similar density on the steel has little effect on the rolling force at a very high reduction.
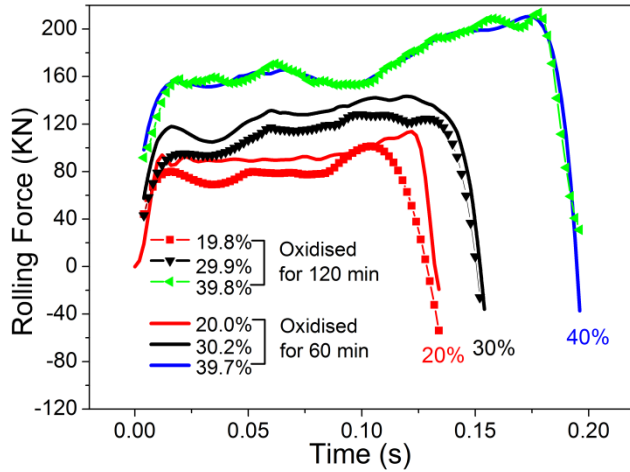
Fig. 5 The rolling forces as a function of time at different reductions when the thickness of the oxide scale differs.

3.2 Oxidation of the stainless steel 445 with grinding or oscillation marks at 1100 °C and the deformation behaviour in hot rolling

Fig. 6 shows the surface profiles of the samples with 45° grinding and oscillation marks. A slab grinder in Baosteel did the work for preparing grinding marks. Fig. 6a shows that the grinding marks are regular and the depth between the peak and the valley is about 70 μm. Fig. 6b shows the surface profile of the sample with oscillation marks where the surface is extremely rough and wavy, and the depth between the peaks and the valleys is not regular.
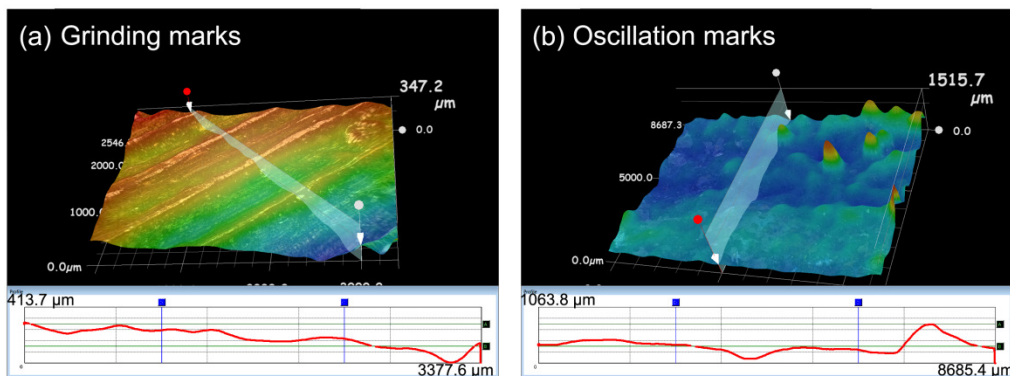

14

Fig. 6 3-D surface profiles of (a) the grinding and (b) oscillation marks on the stainless steel 445

The small samples were cut from one of the rolling specimens with grinding or oscillation marks, which was oxidised at 1100 ℃ for 120 min in humid air.

Fig. 7 shows the surface and the cross section morphology of the oxidised sample with 45 ℃ grinding marks. The grinding marks can still be seen on the oxidised sample, as shown in Fig. 7a. <mark>Although the oxide grew over the grinding marks, the original surface profile was still maintained.</mark> Fig. 7b and c shows some spinels embedded in the fine Cr_2O_3 oxide grains. The oxide composition has not changed by this surface preparation on the stainless steel 445. Fig. 7d shows the cross section of the oxidised sample. The thickness of the oxide scale on the surface with grinding mark was between 2 and 8 µm with an average of 6.1 µm, which is similar to that on the smooth surface.
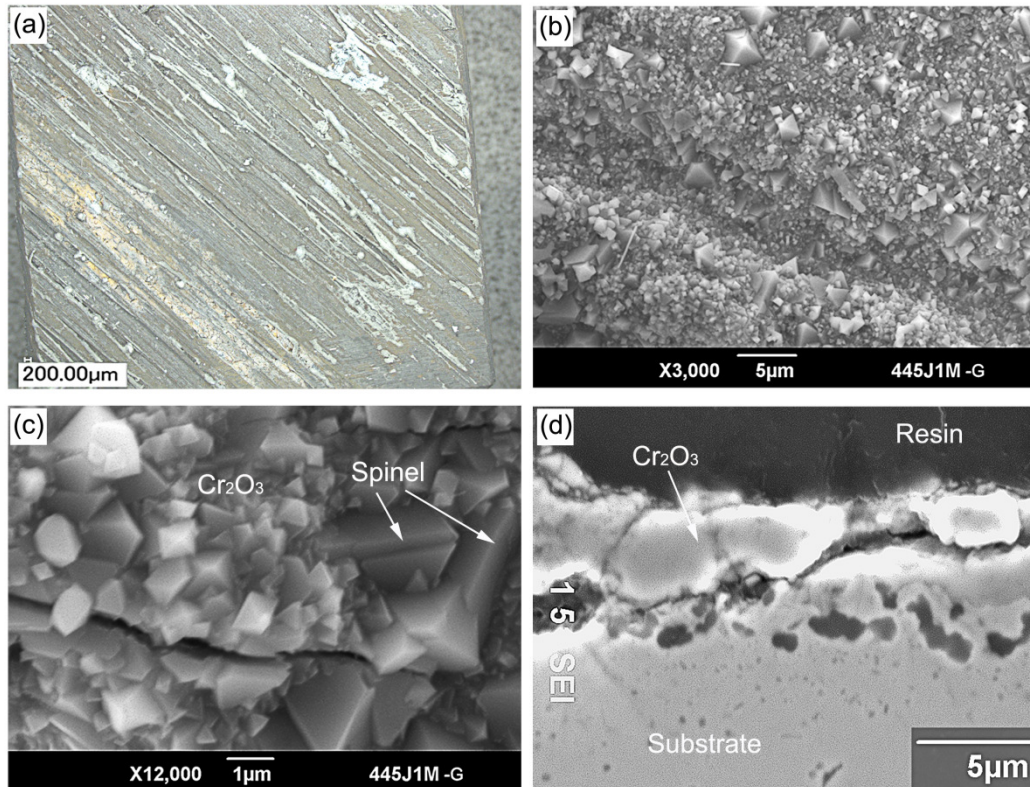
Fig. 7 The surface and cross section morphology of the sample with grinding marks oxidised for 120 min in humid air. (a) oxidised surface, (b) SEM micrograph of the surface morphology, (c) surface morphology in high magnification, and (d) cross section of the oxide scale

Fig. 8 shows the surface and the cross section morphology of the oxidised sample with oscillation marks. The oscillation marks can still be seen on the oxidised sample, as shown in Fig. 8a. The oxide scale appeared non-uniform. Some oxide flakes were spalled off and the steel substrate were exposed, as shown in Fig. 8c. In some regions, the oxide scale was thick which exhibited different structures from that on the smooth surface. Overall, the original surface profile did not change much on the surface with oscillation marks during oxidation. Fig. 8d shows the cross section of the oxidised sample. Besides the Cr_2O_3 scales, oxide nodules comprised of iron oxides with different sizes were formed.
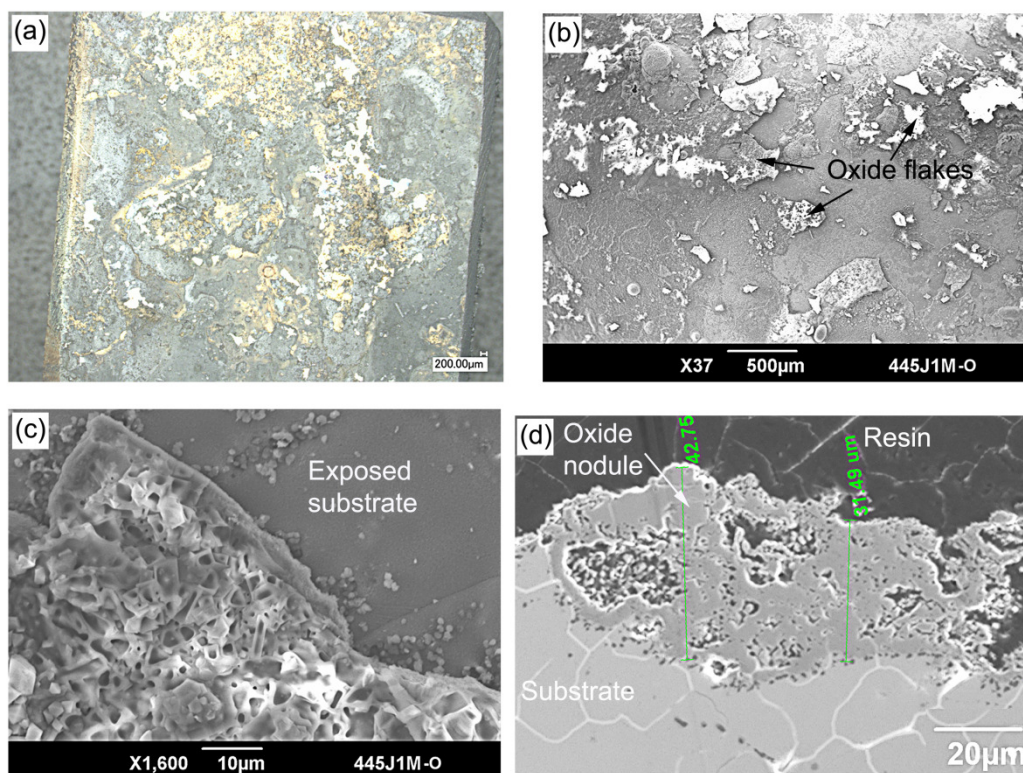
16

Fig. 8 The surface and cross section morphology of the sample with oscillation marks oxidised for 120 min in humid air. (a) oxidised surface, (b) SEM micrograph of the surface morphology, (c) surface morphology in high magnification, and (d) cross section of the oxide scale

Fig. 9 shows the surface morphology of the samples with grinding and oscillation marks at the reductions of 20 and 40% at 1050 ℃ after hot rolling. Fig. 9a1 and b1 show that the grinding and the oscillation marks are still observed when the reduction is 20%. The steel was elongated, and the colour of the surface was not uniform because of the non-uniform oxide scale on the surfaces before hot rolling. Fig. 9a2 and b2 show that the surface become brighter as the specimen is further elongated when the reduction is 40%. The grinding and oscillation marks can hardly be seen at the high reduction. On the surface with originally oscillation marks, the colour appeared non-uniform, as shown in Fig. 9b2, indicating that there existed various

17

oxide thicknesses and the non-uniform distribution of the oxide scale on the rolled specimen surface.
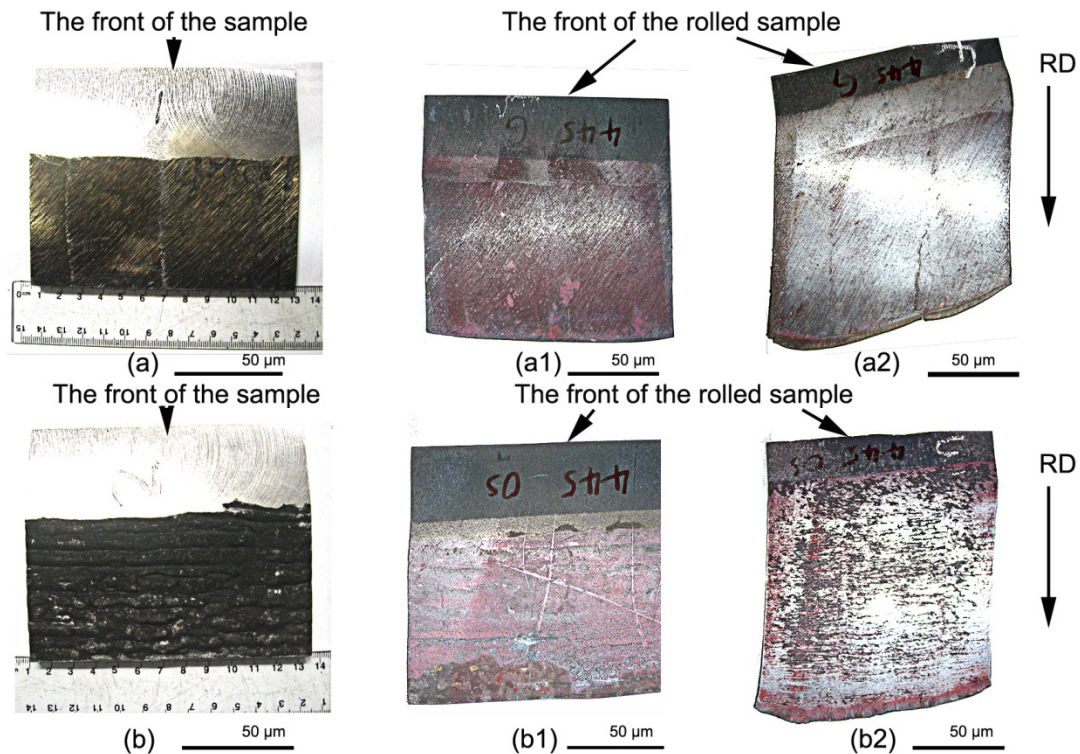

Fig. 9 The specimen with (a) grinding and (b) oscillation marks. (a-b) The specimens before rolling, (a1-b1) the specimens at the reduction of 20% after hot rolling, and (a2-b2) the specimens at the reduction of 40% after hot rolling. The specimens were reheated for 120 min.

Fig. 10 shows the rolling forces as a function of time with different surface preparations at low or high reduction and the corresponding 3-D surface profiles of the rolled specimens. The variation of the rolling forces through the roll gap at the low reduction is not significant. However, the variation of the rolling forces is magnificent at the high reduction when the sample had different surface preparations before hot rolling. Compared to the smooth surface that was used as a comparison, the rolling force for the surface having grinding marks is almost 30% higher at both reductions, and that for the surface having oscillation marks is 200% higher at the reduction of

18

43.5%. The surface with oscillation marks required the largest rolling force and hence, created the largest resistance to the relative motion at this high reduction. Its uneven surface and irregular oxide scale before hot rolling may cause this phenomenon.
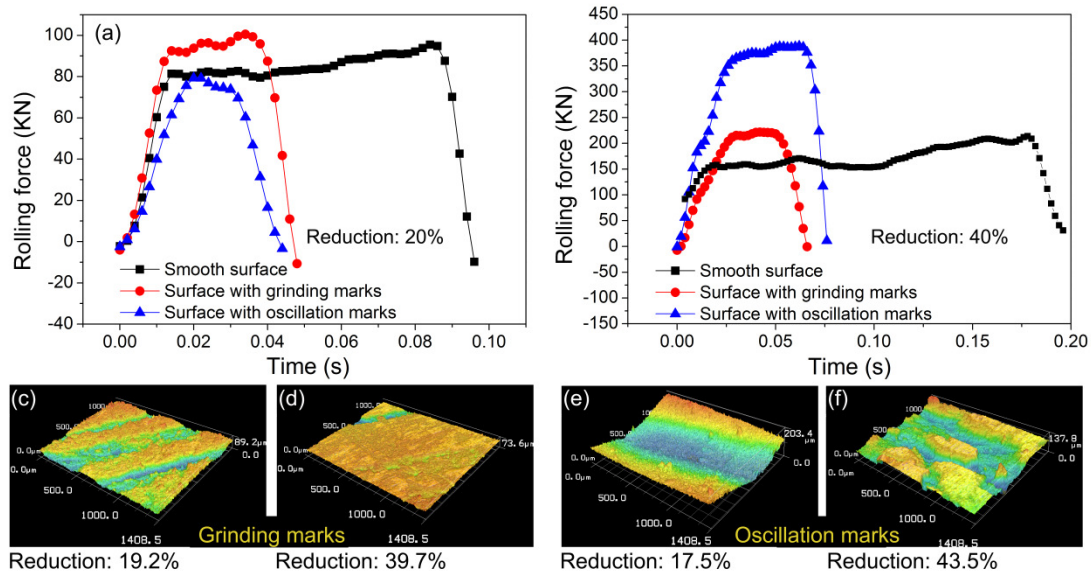

Fig. 10 The rolling forces as a function of time: (a) low reduction of approx. 20%, (b) high reduction of approx. 40%, and 3-D surface profile of rolled sample: (c)(d) reductions of 19.2 and 39.7% for the specimen with grinding marks, and (e)(f) reductions of 17.5 and 43.5% for the specimen with oscillation marks.

Fig. 11 shows the relationship between the coefficient of friction (COF) and the rolling reduction. The COF values were determined by inverse calculations [24]. The effect of the oxide scale thicknesses controlled by oxidation time on COF was compared. Thin oxide scale oxidised for 60 min was 4.1±0.2 µm while thick oxide oxidised for 120 min was 6.0±0.26 µm. When the reduction has not exceeded 30%, the thicker oxide scale leads to a lower COF. However, when the reduction increases to 40%, the difference of COF between the two oxide scale thicknesses is lessening. It can be seen that COF increases more with increased reduction when there was a thicker oxide scale on the stainless steel 445. As the reduction increases from 30 to

19

40%, through thickness cracks were formed more (Fig. 3), therefore, the soft stainless steel substrate could extrude from the oxide scale cracks and touch the roll surface. Moreover, there is a strong metallic bond between the high speed steel (HSS) roll and the steel 445 at high temperature [31], and this can easily cause occurrence of sticking. A slight difference in oxide scale thickness did not influence this deformation behaviour. Sticking may cause higher COF [32]. The grinding marks on the surface of the steel 445 caused higher COF at low and high reductions. The oscillation marks on the surface of the steel 445 had little effect on COF at the low reduction of 17.5%, and the surface was not levelled at the small reduction. However, the COF was extremely high at the reduction of 43.5%.

In hot sheet rolling of low carbon steels, the friction pickup for the carbon steels is rarely to occur due to the thick oxide scale on the sheet surface [33]. Moreover, the surface preparation is not important because of high scaling rate of carbon steels. Stainless steels, however, the sticking, or friction pickup are likely to occur. The parameters during the contact between the roll and the workpiece can directly influence this behaviour. Therefore, some methods were employed to eliminate sticking phenomenon: (a) promoting the formation of the oxide scale, whether it is iron oxides or Cr-rich oxides [10, 31, 32]; (b) adjusting the rolling parameters. For instance, increasing the rolling temperature or rolling speed [10, 33]; (c) adopting appropriate roll material [34, 35]. High speed steel (HSS) roll was more beneficial to prevent sticking compared to a Hi-Cr roll [35]; (d) lubrication. The polyphenylene sulphide (PPS) [33], Zinc dialkyl dithiophosphate (ZDDP) [36], calcium carbonate [37] and calcium sulfonate [38] used as lubricant additives to a base oil were beneficial to prevent surface sticking.

The surface preparation on the stainless steel 445 affects not only the surface appearance but also the coefficients of friction in hot rolling. It would suggest eliminating the defects with fewer and shallower marks on the stainless steel 445 before the slabs are placed for reheating.
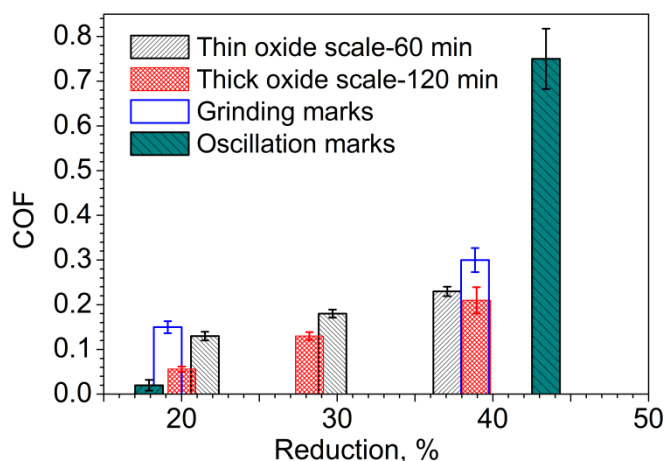

Fig. 11 COF for different surface preparations at different reductions. The stainless steel 445 specimens were rolled at 1050 °C.

4. Conclusions

Oxidation tests of a ferritic stainless steel 445 having different surface preparations were performed in humid air. Hot rolling experiments were carried out on a 2-high Hille 100 experimental mill with surfaces having different oxide scale thickness and marks.

1.   Oxide scale thicknesses of the steel 445 formed at 1100 °C in humid air corresponded to the mass gains which followed a parabolic law. The composition and the density did not change much with increased oxidation time.

2.   The Cr-rich oxide scale on the steel 445 with a thickness of 6.0±0.26 µm displayed through thickness cracks when the reduction was higher than 30% at 1050 °C in hot rolling. The differences in oxide scale thickness affected the rolling forces

and COFs at the rolling reduction less than 30%, but negligibly at the high reduction of 40%.

3.   The oxide scale was not grown thick enough to cover the grinding or oscillation marks on the steel 445 in a reheating environment. On the surface with grinding marks, the composition and the thickness were similar to those on the smooth surface. On the surface with oscillation marks, the oxide scale was not uniform and the compositions of the oxide scale varied and some of the oxide scales were flaked off during cooling process.

4.   The surface having grinding and oscillation marks affected the rolling forces and COF. The surface with grinding marks caused 30% more rolling force during the experiment and a higher COF than the smooth surface. The surface having oscillation marks caused small difference of rolling force at the low reduction but had a magnificent increase at the high reduction of 40%. The COFs varied at different reductions, but valued extremely high at the high reduction.

References

[1] W.L. Roberts, Hot rolling of steel, Marcel Dekker Inc., New York, USA, 1983.
[2] M.F. McGuire, Stainless steel for design engineers, ASM International, Materials Park, OH, USA, 2008.
[3] D.J. Young, High Temperature Oxidation And Corrosion Of Metals, Elsevier, Oxford, 2008.
[4] N. Birks, G.H. Meier, F.S. Pettit, High-Temperature Oxidation of Metals, 2nd ed., Cambridge University Press, Cambridge, 2005.

[5] V.S. Dheeradhada, H. Cao, M.J. Alinger, Oxidation of ferritic stainless steel interconnects: Thermodynamic and kinetic assessment, J. Power Sources, 196 (2011) 1975-1982.

[6] M. Lindgren, S. Siljander, R. Suihkonen, P. Pohjanne, J. Vuorinen, Erosion–corrosion resistance of various stainless steel grades in high-temperature sulfuric acid solution, Wear, 364–365 (2016) 10-21.

[7] I. Kazuhide, I. Tomohiro, O. Hiroki, Nickel-free ferritic stainless steel, Adv. Mater. Processes, (2009 Feb).

[8] D. Peckner, I.M. Bernstein, Handbook of stainless steels, McGraw-Hill Book Company, New York, 1977.

[9] X. Cheng, Z. Jiang, B.J. Monaghan, D. Wei, R.J. Longbottom, J. Zhao, J. Peng, M. Luo, L. Ma, S. Luo, L. Jiang, Breakaway oxidation behaviour of ferritic stainless steels at 1150 °C in humid air, Corros. Sci., 108 (2016) 11-22.

[10] X. Cheng, Z. Jiang, D. Wei, J. Zhao, B.J. Monaghan, R.J. Longbottom, L. Jiang, Characteristics of oxide scale formed on ferritic stainless steels in simulated reheating atmosphere, Surf. Coat. Technol., 258 (2014) 257-267.

[11] M. Reichardt, Surface oxide formation and acid-descaling for stainless steel, Wire Ind., 68 (2001) 503, 505-507.

[12] X. Cheng, Z. Jiang, D. Wei, J. Zhao, B.J. Monaghan, R.J. Longbottom, L. Jiang, High temperature oxidation behaviour of ferritic stainless steel SUS 430 in humid air, Met. Mater. Int., 21 (2015) 251-259.

[13] X. Cheng, Z. Jiang, D. Wei, Effects of oxide scale on hot rolling of an austenitic stainless steel, Int. J. Surface Science and Engineering, 8 (2014) 173-187.

[14] P.A. Munther, J.G. Lenard, The effect of scaling on interfacial friction in hot rolling of steels, J. Mater. Process Tech., 88 (1999) 105-113.

[15] L.H.S.Luong, T. Heijkoop, The influence of scale on friction in hot metal working, Wear, 71 (1981) 93-102.

[16] H. Echsler, S. Ito, M. Schutze, Mechanical properties of oxide scales on mild steel at 800 to 1000 C, Oxid. Met., 60 (2003) 241-269.

[17] R.Y. Chen, Examination of oxide scales of hot rolled steel products, ISIJ Int., 45 (2005) 52-59.

[18] D.B. Wei, J.X. Huang, A.W. Zhang, Z.Y.Jiang, A.K.Tieu, X.Shi, S.H. Jiao, the effect of oxide scale of stainless steels on friction and surface roughness in hot rolling, Wear, 271 (2011) 2417-2425.

[19] D.B. Wei, J.X. Huang, A.W. Zhang, Z.Y. Jiang, A.K.Tieu, X. Shi, S.H. Jiao, X.Y. Qu, Study on the oxidation of stainless steels 304 and 304L in humid air and the friction during hot rolling, Wear, 267 (2009) 1741-1745.

[20] R.Y. Chen, W.Y.D.Yuen, Oxidation of Low-Carbon, Low-Silicon Mild Steel at 450–900°C Under Conditions Relevant to Hot-Strip Processing, Oxid. Met., 57 (2001) 53-78.

[21] J. Tominaga, K. Wakimoto, T. Mori, M. Murakami, T. Yoshimura, Manufacture of Wire Rods With Good Descaling Property, Trans. Iron Steel Inst. Jpn., 22 (1982) 646-656.

[22] W. Sun, A.K. Tieu, Z. Jiang, C. Lu, High temperature oxide scale characteristics of low carbon steel in hot rolling, J. Mater. Process Tech., 155–156 (2004) 1307-1312.

[23] A.M. Huntz, Parabolic laws during high temperature oxidation: relations with the grain size and thickness of the oxide, J. Mater. Sci. Lett., 18 (1999) 1981-1984.

[24] X. Cheng, Z. Jiang, J. Zhao, D. Wei, L. Hao, J. Peng, M. Luo, L. Ma, S. Luo, L. Jiang, Investigation of oxide scale on ferritic stainless steel B445J1M and its tribological effect in hot rolling, Wear, 338–339 (2015) 178-188.

[25] L. Suárez, Y. Houbaert, X.V. Eynde, R. Colás, High temperature deformation of oxide scale, Corros. Sci., 51 (2009) 309-315.

[26] M. Krzyzanowski, J.H. Beynon, D.C.J. Farrugia, Oxide Scale Behavior in High Temperature Metal Processing, Wiley, Hoboken, 2010.

[27] M. Krzyzanowski, J.H. Beynon, Modelling the behaviour of oxide scale in hot rolling, ISIJ Int., 46 (2006) 1533-1547.

[28] H. Utsunomiya, K. Hara, R. Matsumoto, A. Azushima, Formation mechanism of surface scale defects in hot rolling process, CIRP Ann.-Manuf. Techn., 63 (2014) 261-264.

[29] H. Utsunomiya, S. Doi, K.-i. Hara, T. Sakai, S. Yanagi, Deformation of oxide scale on steel surface during hot rolling, CIRP Ann.-Manuf. Techn., 58 (2009) 271-274.

[30] X. Cheng, Z. Jiang, D. Wei, L. Hao, J. Zhao, L. Jiang, Oxide scale characterization of ferritic stainless steel and its deformation and friction in hot rolling, Tribol. Int., 84 (2015) 61-70.

[31] X. Cheng, Z. Jiang, B. Kosasih, H. Wu, S. Luo, L. Jiang, Influence of Cr-Rich Oxide Scale on Sliding Wear Mechanism of Ferritic Stainless Steel at High Temperature, Tribol. Lett., 63 (2016) 1-13.

[32] Y. Hidaka, S. Lida, Influence of surface oxide scale of Fe Cr alloy on tool lubrication characteristic during hot rolling, Tetsu To Hagane, 96 (2010) 156-161.

[33] A. Azushima, Tribology in Hot Sheet Rolling, Tribology in Sheet Rolling Technology, Springer International Publishing, Cham, 2016, pp. 255-330.

[34] W. Jin, J.Y. Choi, Y.Y. Lee, Nucleation and growth process of sticking particles in ferritic stainless steel, ISIJ Int., 40 (2000) 789-793.

[35] W. Jin, J.Y. Choi, Y.Y. Lee, Effect of roll and rolling temperatures on sticking behavior of ferritic stainless steels, ISIJ Int., 38 (1998) 739-743.

[36] L. Hao, Z. Jiang, X. Cheng, J. Zhao, D. Wei, L. Jiang, S. Luo, M. Luo, L. Ma, Effect of Extreme Pressure Additives on the Deformation Behavior of Oxide Scale during the Hot Rolling of Ferritic Stainless Steel Strips, Tribol. T., 58 (2015) 947-954.

[37] N. Shimotomai, H. Ihara, H. Nanao, A study of hot rolling oil with calcium carbonate for stainless steel process, Tribology Online, 3 (2010) 181-186.

[38] K. Gotoh, T. Shibahara, K. Takeuchi, Effects of overbased organic metal salts on lubricity in hot working, Tetsu To Hagane, 84 (1998) 502-509.